1,3-Cyclopentanediyl Diradicals: Substituent and Temperature Dependence of Triplet−Singlet Intersystem Crossing

Fumio Kita,[†] Waldemar Adam,*,[†] Paul Jordan,[§] Werner M. Nau,[‡] and Jakob Wirz*,[‡]

Contribution from the Institut für Organische Chemie der Universität Würzburg, Am Hubland, D-97074 Würzburg, Germany, and the Institut für Physikalische Chemie and the Universitätsrechenzentrum, Universität Basel, Klingelbergstrasse 80, CH-4056 Basel, Switzerland

Abstract: The lifetimes of 33 1,3-diaryl-1,3-cyclopentanediyl triplet diradicals were determined by laser flash photolysis of the corresponding azoalkane precursors. The first-order decay rate constants range from 0.8 to 16.7×10^5 s^{-1} in degassed solution at 294 K and exhibit a systematic, but nonlinear dependence on Brown's σ^+ substituent constants. Analysis of spin−orbit coupling in terms of the two-electrons-in-two-orbitals model indicates that the electronic effect on the rates of intersystem crossing operates by influencing the weight of ionic contributions in the lowest singlet state wave functions of the diradicals. Counter to intuition, but in agreement with the prediction by the model, push−pull substitution does not enhance the ionic contribution. Arrhenius parameters, $E_a = 2-6$ kcal mol^{-1} and $A = 10^7-10^{10}$ s^{-1}, were determined from the temperature dependences of the decay rate constants. A sensitive statistical test is used to establish that the Arrhenius parameters exhibit enthalpy−entropy compensation, that is, an approximate isokinetic relationship.

Introduction

Diradicals are ephemeral because their bifunctionality generally entails intramolecular paths for stabilization. For triplet diradicals these reactions are, however, impeded by a "spin barrier", as *intersystem crossing* (ISC) to the singlet state is required. This step usually determines the lifetime of triplet diradicals, $k_{ISC} = \tau_{obsd}^{-1}$. *Spin−orbit coupling* (SOC)[1−7] and *hyperfine coupling*[8] are primarily responsible for ISC in diradicals. Hyperfine coupling becomes important for 1,*n*-

diradicals connected by extended chains ($n \gtrsim 7$).[9] The present study deals with substituent effects on the lifetimes of 1,3-diradicals, for which SOC is the dominant mechanism inducing ISC.

Lifetimes of numerous triplet diradicals have been determined.[10] Nevertheless, a comparison with theoretical predictions for substituent effects is difficult, because calculated ISC rates depend both on electronic and on geometrical factors such as the relative orientation of the radical centers and of the tether.[2] For flexible systems, SOC matrix elements need to be evaluated for a distribution of molecular conformations and averaged over wave functions of internal rotation.[11] With the goal to determine electronic substituent effects in model systems with restricted conformational freedom, we investigated the diaryl-substituted 1,3-cyclopentanediyls **1** and **2** (Scheme 1), in which the radical centers are embedded in a five-membered ring.[12] In this series the substituent effects on ISC rate constants follow a remarkably simple pattern, which confirms predictions derived from a model of two electrons in two orbitals.[3] Moreover, the variation of the ISC rate constants with temperature reveals the interplay of substituent effects on SOC and on the thermal barrier for ISC.

Results

Diradicals **1** and **2** were generated by irradiation of the corresponding azoalkanes **3** and **4**, which were synthesized by

† Universität Würzburg.
‡ Institut für Physikalische Chemie, Basel.
§ Universitätsrechenzentrum, Basel.

(1) (a) McGlynn, S. P.; Azumi, T.; Kinoshita, M. In *Molecular Spectroscopy of the Triplet State*; Prentice Hall: Englewood Cliffs, 1969; Chapter 5. (b) Langhoff, S. R. In *Modern Theoretical Chemistry*; Schaefer, H. F., III, Ed.; Plenum: New York, 1977; Vol. 4. (c) Levine, I. N. In *Quantum Chemistry*; Allyn and Bacon: Newton, MA, 1983; p 281.

(2) Salem, L.; Rowland, C. *Angew. Chem., Int. Ed. Engl.* **1972**, *11*, 92.

(3) (a) Bonačić-Koutecký, V.; Koutecký, J.; Michl, J. *Angew. Chem., Int. Ed. Engl.* **1987**, *26*, 170. (b) Michl, J.; Bonačić-Koutecký, V. In *Electronic Aspects of Organic Photochemistry*; John Wiley & Sons: New York, 1990; p 169. (c) Michl, J. In *Theoretical and Computational Models for Organic Chemistry*; Formosinho, S. J., Czismadia, I. G., Arnaut, L. G., Eds.; Kluwer: Dordrecht, The Netherlands, 1991; p 207. (d) Michl, J. *J. Mol. Struct. (THEOCHEM)* **1992**, *260*, 299. (e) Michl, J. *J. Am. Chem. Soc.* **1996**, *118*, 3568.

(4) (a) Zimmermann, H. E.; Kutateladze, A. G.; Maekawa, Y.; Mangette, J. E. *J. Am. Chem. Soc.* **1994**, *116*, 9795. (b) Zimmermann, H. E.; Kutateladze, A. G. *J. Org. Chem.* **1995**, *60*, 6008. (c) Zimmermann, H. E.; Kutateladze, A. G. *J. Am. Chem. Soc.* **1996**, *118*, 249.

(5) (a) Minaev, B. F.; Jonsson, D.; Norman, P.; Ågren, H. *Chem. Phys.* **1995**, *194*, 19. (b) Knuts, S.; Minaev, B. F.; Vahtras, O.; Aagren, H. *Int. J. Quantum Chem.* **1995**, *55*, 23.

(6) (a) Böckmann, M.; Klessinger, M. *Angew. Chem., Int. Ed. Engl.* **1996**, *35*, 2502. (b) Böckmann, M.; Klessinger, M.; Zerner, M. C. *J. Phys. Chem.* **1996**, *100*, 10570. (c) Klessinger, M. In *Theoretical and Computational Chemistry, Vol. 5: Theoretical Organic Chemistry*; Párkányi, C., Ed.; Elsevier: Amsterdam, The Netherlands, 1998.

(7) (a) Furlani, T. R.; King, H. F. *J. Chem. Phys.* **1985**, *82*, 5577. (b) Carlacci, L.; Doubleday, C., Jr.; Furlani, T. R.; King, H. F.; McIver, J. W., Jr. *J. Am. Chem. Soc.* **1987**, *109*, 5323. (c) Caldwell, R. A.; Carlacci, L.; Doubleday, C. E., Jr.; Furlani, T. R.; King, H. F.; McIver, J., Jr. W. *J. Am. Chem. Soc.* **1988**, *110*, 6901. (d) Havlas, Z.; Downing, J. D.; Michl, J. *J. Phys. Chem.* **1998**, *102*, 5681.

(8) (a) De Kanter, F. F. J.; Den, Hollander, J. A.; Huizerm, A. H.; Kaptein, R. *Mol. Phys.* **1977**, *34*, 857. (b) De Kanter, F. J. J.; Kaptein, R. *J. Am. Chem. Soc.* **1982**, *104*, 4759. (c) Turro, N. J.; Kräutler, B. *Acc. Chem. Res.* **1980**, *13*, 369.

(9) Doubleday, C., Jr.; Turro, N. J.; Wang, J.-F. *Acc. Chem. Res.* **1989**, *22*, 199.

(10) (a) Caldwell, R. A. *Pure Appl. Chem.* **1984**, *56*, 1167. (b) Johnston, L. J.; Scaiano, J. C. *Chem. Rev.* **1989**, *89*, 521. (c) Adam, W.; Grabowski, S.; Wilson, R. M. *Acc. Chem. Res.* **1990**, *23*, 165. (d) Caldwell, R. A. In *Kinetics and Spectroscopy of Carbenes and Biradicals*; Platz, M. S., Ed.; Plenum: New York, 1990; p 117. (e) Ichinose, N.; Mizuno, K.; Otsuji, Y.; Caldwell, R. A.; Helms, A. M. *J. Org. Chem.* **1998**, *63*, 3176.

(11) Morita, A.; Kato, S. *J. Phys. Chem.* **1993**, *97*, 3298.

(12) Preliminary publications: (a) Adam, W.; Fröhlich, L.; Nau, W. M.; Wirz, J. *J. Am. Chem. Soc.* **1993**, *115*, 9824. (b) Kita, F.; Nau, W. M.; Adam, W.; Wirz, J. *J. Am. Chem. Soc.* **1995**, *117*, 8670.

Scheme 1
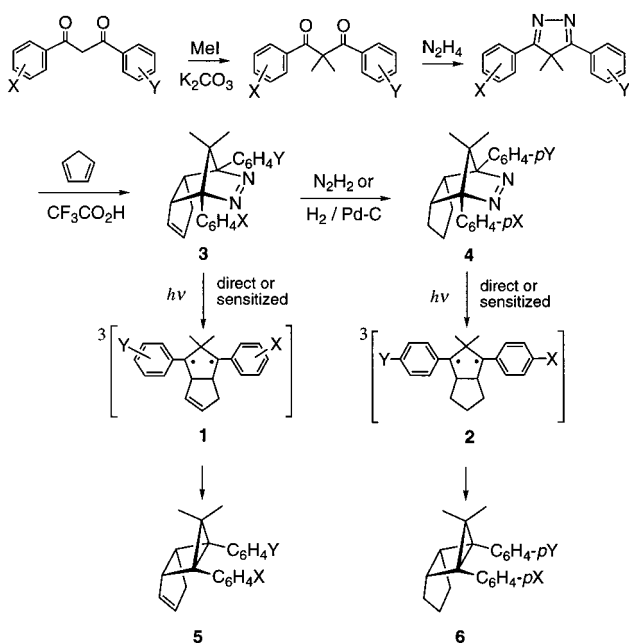
the general route shown in Scheme 1. Unless previously documented,[13] synthetic details and compound identification are given as Supporting Information. The azoalkanes exhibit a weak n,π^* transition ($\epsilon \sim 150$ M^{-1} s^{-1}) around 360 nm, and irradiation affords the *endo* housanes **5** and **6** in quantitative yields, except for the amino- and nitro-substituted azoalkanes, which form secondary photoproducts upon prolonged irradiation.

Degassed benzene solutions of azoalkanes **3** and **4** were pumped with a 351-nm excimer laser pulse (25 ns, XeF), and in most cases the transient absorbance was monitored at 320 nm. Azoalkanes **3** and **4** undergo efficient ISC to the triplet manifold.[14] Therefore, triplet sensitization is not required and the triplet diradicals **1** and **2** are readily generated by direct flash photolysis of the azo precursors in solution. Two sequential processes, the denitrogenation of the triplet azoalkanes and the decay of the triplet diradicals, are manifested by dual exponential decay traces in kinetic flash photolysis (Figure 1). Alternatively, the triplet diradicals **1** and **2** were generated by triplet sensitization of the azoalkanes with benzophenone ($\lambda_{exc} = 308$ nm, XeCl excimer laser). The lifetimes of the triplet diradicals determined in this way agreed ($\pm 5\%$) with those measured by direct flash photolysis.

Evidence for the assignment of the first transient intermediate to the excited triplet state of the azo compounds **3** or **4** has been given previously.[14b] The assignment of the slower decays to the triplet diradicals **1** or **2** is based on the following observations: (i) The transient UV absorption spectra are similar to those of the corresponding benzyl ($\lambda_{max} = 316$ nm, $\epsilon = 8800$ cm^{-1} M^{-1})[15] and cumyl ($\lambda_{max} = 316$ nm)[16] radicals.[17] (ii) Product studies have shown that the housanes are formed quantitatively by both direct and sensitized irradiation.[13b,d,e] (iii)

The triplet diradicals were identified by their ESR spectra,[13d,18] which persist for hours in rigid glassy media at 77 K. (iv) The diradical lifetimes are not affected by the addition of the triplet quencher *trans*-piperylene in up to 0.1 M concentration. (v) Scavenging of the triplet diradicals by molecular oxygen, presumably to afford the corresponding peroxide trapping products,[12a] occurs with rate constants in the range $0.4-2.7 \times 10^9$ M^{-1} s^{-1}, depending on the substituents X and Y. (vi) The reaction rates are independent of azoalkane concentration. (vii) The Arrhenius pre-exponential factors are small, $\log(A/\text{s}^{-1}) = 7-10$ (vide infra), which is characteristic for spin-forbidden processes.

For derivatives with a nitro substituent, the azo n,π^* bands of **3** and **4** overlapped with end absorption by the nitrophenyl chromophore. Solutions of these compounds with adequate absorbance at the excitation wavelength of 351 nm ($A \cong 0.4$) were opaque at 320 nm, and the diradicals could not be monitored at this wavelength. However, transient absorption spectra of these diradicals revealed strong absorption bands at ~ 355 and 580 nm, which are attributed to the *p*-nitrobenzyl chromophore. Similar spectra were observed upon irradiation of azoalkane **3** (X = Y = *p*-NO$_2$) in an EPA glass at 77 K (Figure 2). Although optical spectra of *p*-nitrobenzyl radicals have been previously recorded,[19b,e,f] the spectral range was limited to the UV region, such that the strong absorption at 580 nm has apparently escaped detection prior to the present work. To ascertain this inference, we generated *p*-nitrobenzyl radicals independently by 308-nm flash photolysis of the so-called Barton-PTOC (pyridine-2-thione-*N*-oxycarbonyl) precursor[20] in acetonitrile and indeed found them to exhibit about equally strong absoption at 330 and 560 nm, in agreement with the diradical spectra.

The lifetimes of diradicals **1** and **2** range from 0.6 to 12 μs in degassed solutions (Table 1). Solvent effects were found to be of minor importance; for example, the lifetimes of the triplet diradical **2** (X = Y = *p*-NO$_2$) were essentially the same in benzene (11.4 ± 0.6 μs) and acetonitrile (12.0 ± 0.5 μs). Lifetime data for hydroxyl-substituted azoalkanes were determined in acetonitrile for solubility reasons. The ISC rates of the symmetrically disubstituted diradicals **1** with a C–C double bond in the fused five-membered ring were generally higher by a factor of 1.8 ± 0.1 than those of the C–C saturated analogues **2** (Table 1).

The temperature dependences of the ISC rate constants in degassed benzene solution were determined in the range 10–50 °C (Table S1, Supporting Information). The rate constants

(13) (a) Beck, K.; Hünig, S. *Chem. Ber.* **1987**, *120*, 477. (b) Adam, W.; Harrer, H. M.; Nau, W. M.; Peters, K. *J. Org. Chem.* **1994**, *59*, 3786. (c) Nau, W. M.; Harrer, H. M.; Adam, W. *J. Am. Chem. Soc.* **1994**, *116*, 10972. (d) Adam, W.; Kita, F.; Harrer, H. M.; Nau, W. M.; Zipf, R. *J. Org. Chem.* **1996**, *61*, 7056. (e) Adam. W.; Harrer, H. M.; Kita, F.; Korth, H.-G.; Nau, W. M. *J. Org. Chem.* **1997**, *62*, 1419.

(14) (a) Adam, W.; Nau, W. M.; Sendelbach, J. S. *J. Am. Chem. Soc.* **1994**, *116*, 7049. (b) Adam, W.; Fragale, G.; Klapstein, D.; Nau, W. M.; Wirz, J. *J. Am. Chem. Soc.* **1995**, *117*, 12578.

(15) (a) Jordan, J. E.; Pratt, D. W.; Wood, D. E. *J. Am. Chem. Soc.* **1974**, *96*, 5589. (b) Neta, P.; Behar, D. *J. Am. Chem. Soc.* **1980**, *102*, 4798. (c) Claridge, R. F. C.; Fischer, H. *J. Phys. Chem.* **1983**, *87*, 1960. (d) Tokumura, K.; Nosaka, H.; Ozaki, T. *Chem. Phys. Lett.* **1990**, *169*, 321. (e) Tokumura, K.; Ozaki, T.; Nosaka, H.; Saigusa, Y.; Itoh, M. *J. Am. Chem. Soc.* **1991**, *113*, 4974. (f) Mayouf, A. M.; Lemmetyinen, H.; Koskikallio, J. *J. Photochem. Photobiol., A* **1993**, *70*, 215–221.

(16) (a) Brand, U.; Hippler, H.; Lindemann, L.; Troe, J. *J. Phys. Chem.* **1990**, *94*, 6305. (b) Boury, V. W.; Ingold, K. U. *J. Am. Chem. Soc.* **1992**, *114*, 4992. (c) Faria, J. L.; Steenken, S. *J. Phys. Chem.* **1992**, *96*, 10869.

(17) The bands of the diradicals are broad and the band maxima lie at somewhat shorter wavelengths than the 0–0 transitions of the corresponding monoradicals.

(18) Adam, W.; Fröhlich, L.; Nau, W. M.; Korth, H.-G.; Sustmann, R. *Angew. Chem., Int. Ed. Engl.* **1993**, *32*, 1339.

(19) (a) Jordan, J. E.; Pratt, D. W.; Wood, D. E. *J. Am. Chem. Soc.* **1974**, *96*, 5589. (b) Neta, P.; Behar, D. *J. Am. Chem. Soc.* **1980**, *102*, 4798. (c) Claridge, R. F. C.; Fischer, H. *J. Phys. Chem.* **1983**, *87*, 1960. (d) Tokumura, K.; Nosaka, H.; Ozaki, T. *Chem. Phys. Lett.* **1990**, *169*, 321. (e) Tokumura, K.; Ozaki, T.; Nosaka, H.; Saigusa, Y.; Itoh, M. *J. Am. Chem. Soc.* **1991**, *113*, 4974. (f) Mayouf, A. M.; Lemmetyinen, H.; Koskikallio, J. *J. Photochem. Photobiol., A* **1993**, *70*, 215–221.

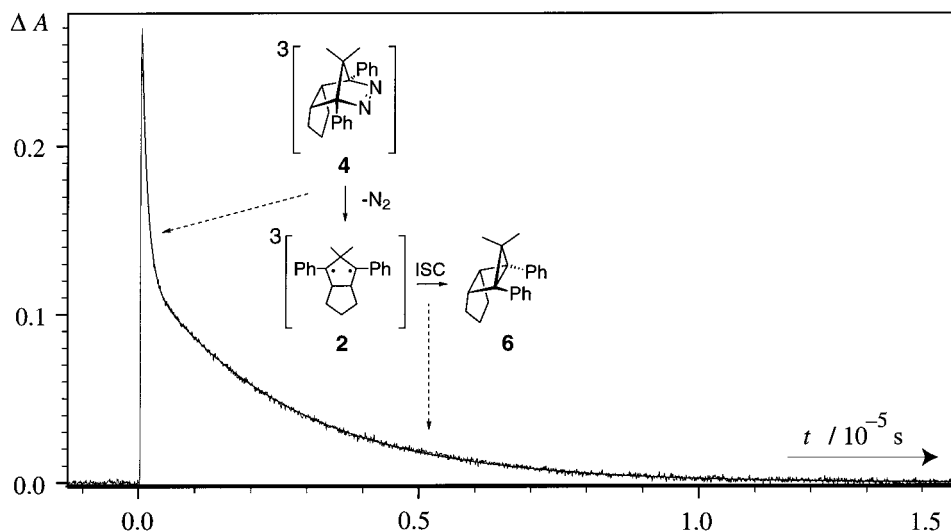(20) Barton, D. H. R.; Ferreira, J. A. *Tetrahedron* **1996**, *52*, 9347.

Figure 1. Transient absorbance changes observed at 320 nm by flash photolysis of a solution of azoalkane **4** (X = Y = H) in degassed benzene at 20.5 °C with a XeF excimer laser (351 nm).
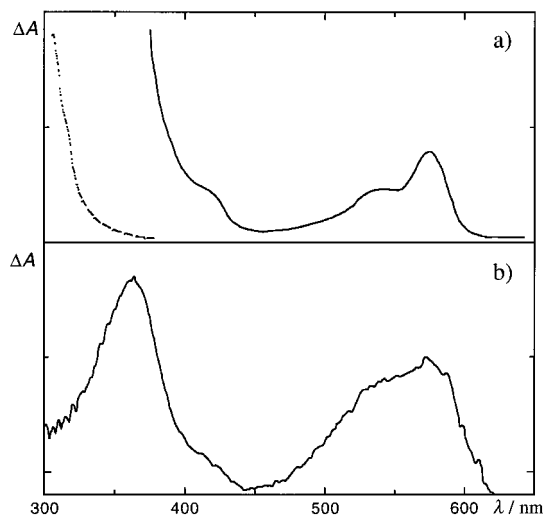

Figure 2. Absorption spectra of triplet diradical **1** (X = Y = *p*-NO$_2$); (a) spectrum in EPA matrix at 77 K (the dotted line shows the absorption of the azoalkane precursor **3**) and (b) transient spectrum observed with a time delay of 1 μs after nanosecond laser flash photolysis of **3** (X = Y = *p*-NO$_2$) in degassed benzene solution at ambient temperature.
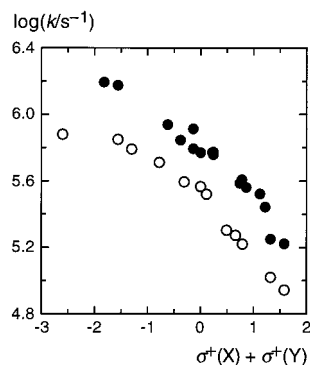

Figure 3. Intersystem-crossing rate constants (k_{ISC}) of the triplet diradicals **1** (●) and **2** (○) versus the sum of the substituent parameters σ^+ of the substituents X and Y.

obeyed the Arrhenius law (eq 1). On the basis of the experience that *relative* errors in the experimental rate constants are constant, the activation parameters *A* and E_a given in Table 1 were determined by linear regression of the logarithmic form

of the Arrhenius equation.

$$k_{ISC} = A \exp(-E_a/RT) \qquad (1)$$

Discussion

Triplet diradicals **1** and **2** react quantitatively by cyclization to the housanes **5** and **6** (Scheme 1). This spin-forbidden reaction requires thermal activation energy as revealed by the temperature dependence of the rate constants k_{ISC}, in particular by their persistence for hours at 77 K. Accordingly, two factors are considered to influence the observed triplet lifetimes: first, a "transmission factor" accounting for the requirement of spin flip along the reaction coordinate and, second, a small but significant thermal barrier toward ring closure.[21] Following these considerations, we factorize the Arrhenius equation into two contributions, a transmission factor A_{SOC} accounting for the spin barrier and the expression $A_\Delta \exp(-E_a/RT)$ reflecting the thermal barrier (eq 2). We will first give a simple empirical treatment

$$k_{ISC} = A_{SOC}A_\Delta \exp(-E_a/RT) \qquad (2)$$

of the lifetime data by means of substituent parameters. In a second step, we will demonstrate that the substituent effects on the lifetimes at room temperature can be adequately described considering only SOC.[22] Finally, we will consider the temperature dependences of the triplet lifetimes that are described by the remaining, "conventional" parameters of the Arrhenius eq 2, A_Δ and E_a.

Empirical Analysis. Electron acceptors (NO$_2$ or CN) reduce the rate of ISC relative to the parent system (lengthen the triplet lifetime), while electron donors (MeO or NH$_2$) accelerate ISC in the triplet diradicals **1** and **2** (shorten their lifetimes). These electronic substituent effects are general; they hold for substitution at the *para* and *meta* positions, both for the symmetrical (X = Y) and nonsymmetrical (X ≠ Y) aryl substitution patterns, and are largely independent of solvent polarity.

(21) Adam, W.; Platsch, H.; Wirz, J. *J. Am. Chem. Soc.* **1989**, *111*, 6896.

(22) The mechanism responsible for the spin flip in the 1,3-diradicals **1** and **2** is SOC. The lifetimes of several triplet diradicals **1** and **2**, which include the longest- and shortest-lived derivatives and those with heavy atoms, have been measured at various magnetic field strengths up to 5000 G, but no effect was observed within an error of ±5%. These results preclude any significant contributions from hyperfine coupling, the alternative mechanism for inducing ISC (ref 8).

Table 1. Triplet Lifetimes ($^3\tau$) of the Diradicals **1** and **2** and Calculated Covalent (γ_{AB}) and Polar (δ_{AB}) Perturbations in the Planar Model Diradicals **7**

diradical	substituents[a]		$^3\tau^b$ (ns)	$E_a{}^c$ (kcal mol⁻¹)	log $(A/s^{-1})^c$	$\sigma^+(X)^d$	$\gamma_{AB}{}^e$ (10^{-2} eV)	$\delta_{AB}{}^f$ (eV)
	X	Y						
1	p-I	p-I	570 ± 10			0.14	−3.43	0
	p−OH	p−OH	640 ± 40[g]	3.8 ± 0.3	9.0 ± 0.2	−0.91	−6.05	0
	p−OMe	p−OMe	670 ± 10[h]	1.7 ± 0.1	7.5 ± 0.5	−0.78	−6.13	0
	p-Br	p-Br	960 ± 10[h]	3.6 ± 0.1	8.7 ± 0.1	0.15	−3.74	0
	p-Me	p-Me	1150 ± 30[h]	1.8 ± 0.1	7.3 ± 0.1	−0.31	−4.78	0
	p-F	p-F	1220 ± 50[h]	1.9 ± 0.2	7.4 ± 0.2	−0.07	−4.91	0
	p-OAc	p-OAc	1430 ± 60	3.1 ± 0.2	8.2 ± 0.2	−0.19	−4.91	0
	m-I	m-I	1440 ± 30			0.35	−3.59	0
	m-Me	m-Me	1610 ± 160	2.0 ± 0.5	7.3 ± 0.4	−0.07	−4.27	0
	m-OH	m-OH	1680 ± 220[g]	3.0 ± 0.6	8.0 ± 0.5	0.12	−4.07	0
	H	H	1700 ± 40[h]	1.8 ± 0.2	7.1 ± 0.1	0.00	−4.23	0
	p-Cl	p-Cl	1700 ± 20[h]	2.5 ± 0.1	7.6 ± 0.1	0.11	−4.23	0
	m-OMe	m-OMe	1740 ± 200			0.12	−4.22	0
	m-OAc	m-OAc	2460 ± 180	3.8 ± 0.4	8.5 ± 0.3	0.39	−3.59	0
	m-Cl	m-Cl	2600 ± 150	3.2 ± 0.3	8.0 ± 0.2	0.37	−3.36	0
	m-CF₃	m-CF₃	2750 ± 430	2.9 ± 0.8	7.7 ± 0.6	0.43	−3.07	0
	m-CN	m-CN	3000 ± 120	3.4 ± 0.2	8.1 ± 0.2	0.56	−3.44	0
	p-CF₃	p-CF₃	3600 ± 140	2.7 ± 0.2	7.5 ± 0.2	0.61	−2.62	0
	p-CN	p-CN	5620 ± 150	3.5 ± 0.2	7.9 ± 0.1	0.66	−3.31	0
	p-NO₂	p-NO₂	6150 ± 300[h]	5.1 ± 0.1	9.0 ± 0.1	0.79	−2.11	0
	p-OMe	p-NO₂	1840 ± 40[i]				−3.78	0.579
2	p-NH₂	p-NH₂	1320 ± 20	5.2 ± 0.2	9.8 ± 0.1	−1.30	−5.77	0
	p-OMe	p-OMe	1420 ± 20	4.4 ± 0.2	9.2 ± 0.1	−0.78	−5.73	0
	p-NH₂	H	1620 ± 50	3.6 ± 0.2	8.5 ± 0.1	−1.30	−4.88	−0.169
	p-OMe	H	1940 ± 30	2.8 ± 0.1	7.8 ± 0.1	−0.78	−4.66	−0.096
	p-OMe	H	2000 ± 90[g]					
	p-Me	H	2540 ± 60	2.6 ± 0.1	7.5 ± 0.1	−0.31	−4.05	−0.031
	H	H	2710 ± 90	3.6 ± 0.2	8.2 ± 0.1	0.00	−3.83	0
	p-Cl	H	3020 ± 50	3.2 ± 0.1	7.9 ± 0.1	0.11	−3.75	0.103
	p-CO₂Me	H	4970 ± 50	3.6 ± 0.1	8.0 ± 0.1	0.49	−3.03	0.260
	p-CN	H	5330 ± 50	3.6 ± 0.2	8.0 ± 0.1	0.66	−3.25	0.262
	p-CN	H	5280 ± 110[g]					
	p-NO₂	H	6030 ± 500			0.79	−2.55	0.476
	p-CN	p-CN	9550 ± 140	4.6 ± 0.1	8.5 ± 0.1	0.66	−2.91	0
	p-NO₂	p-NO₂	11400 ± 600	6.1 ± 0.2	9.5 ± 0.1	0.79	−1.71	0
	p-NO₂	p-NO₂	12000 ± 500[g]					

[a] The triplet diradicals were generated from the corresponding azoalkanes **3** or **4** by flash photolysis with a XeF excimer laser (351 nm). [b] Mean value and standard error of samples of about twenty individual measurements in degassed benzene solutions at 20.0 °C. [c] Mean values and standard errors of the Arrhenius parameters. Temperature range 10−50 °C, 5−10 measurements at each temperature. [d] Brown's substituent parameters from ref 23. [e] Covalent perturbation in diradicals **7** calculated by AM1; for *meta*-disubstituted compounds, the conformation with both substituents on the side of the methylene bridge was chosen. The values were corrected for the underrated *through−space* interaction by AM1, cf. footnote 32. [f] Polar perturbation in diradicals **7** (AM1); in the monosubstituted diradicals **2** orbital A is localized on the unsubstituted benzyl radical. [g] Values measured at 20 °C in degassed acetonitrile. [h] See also ref 12a. [i] A ∼1:1 mixture of two regioisomers; see also ref 12b.

These trends are nicely illustrated by a Hammett plot of the ISC rate constants versus the sum of Brown's substituent constants[23] σ^+ for the two substituents X and Y of the two sets of diradicals **1** and **2** (Figure 3). The two series clearly follow a systematic, albeit nonlinear trend.[24] Diradicals carrying bromine or iodine substituents, which are known to enhance SOC through the so-called internal heavy-atom effect,[25] clearly fall out of line and were omitted from this plot.

(23) Hantsch, C.; Leo, A.; Taft, R. W. *Chem. Rev.* **1991**, *91*, 165.

(24) A correlation between ISC rates and aryl substituent parameters has been previously described for unsymmetrical Norrish-Type-II diradicals in nonpolar solvents, generated photochemically from γ-phenylbutyrophenone derivatives (ref 10a,d). In the polar solvent methanol, the substituents had essentially no influence on the triplet diradical lifetimes.

(25) (a) Kavarnos, G.; Cole, T.; Scribe, P.; Dalton, J. C.; Turro, N. J. *J. Am. Chem. Soc.* **1971**, *93*, 1033. (b) Cowan, D. O. M.; Drisko, R. L. in *Elements of Organic Photochemistry*; Plenum: New York, 1975, 250. (c) Miller, J. C.; Meek, J. S.; Strickler, S. J. *J. Am. Chem. Soc.* **1977**, *99*, 8175. (d) Mizuno, K.; Ichinose, N.; Otsuji, Y.; Caldwell, R. A. *J. Am. Chem. Soc.* **1985**, *107*, 5797. (e) Zimmt, M. B.; Doubleday, C., Jr.; Turro, N. J. *Chem. Phys. Lett.* **1987**, *134*, 549. (f) Fisher, J. J.; Michl, J. *J. Am. Chem. Soc.* **1987**, *109*, 583. (g) Ermler, W. C.; Ross, R. B.; Christiansen, P. A. *Adv. Quantum Chem.* **1988**, *19*, 139. (h) Caldwell, R. A.; Jacobs, L. D.; Furlani, T. R.; Nalley, E. A.; Laboy, J. *J. Am. Chem. Soc.* **1992**, *114*, 1623. (i) Khudyakov, I. V.; Serebrennikov, Y. A.; Turro, N. J. *Chem. Rev.* **1993**, *93*, 537.

The Two-Electrons-In-Two-Orbitals Model for SOC. The first detailed theoretical analysis of the factors that influence SOC in homosymmetric diradicals was carried out by Salem and Rowland.[2] These authors found a dependence on (i) the relative orientation of the orbitals at the radical sites, (ii) the distance between the radical centers, (iii) the atom types, and (iv) the electronic structure of the lowest singlet state, namely, its zwitterionic character. A more elaborate description of the electronic structure of diradicaloids in terms of the two-electrons-in-two-orbitals active space was formulated by Michl and co-workers.[3] Their treatment, which is employed here, covers homosymmetric and nonsymmetric diradicals within the same framework.

As a basis set, fully localized nonbonding molecular orbitals A and B are chosen for minimal interorbital and maximal intraorbital electronic repulsion. If only the through-space interaction is taken into account, the fully localized orbitals correspond to the separate radical (benzyl) orbitals. When the through-bond interaction is also considered, these orbitals spread over the adjacent σ bonds. The extent of this delocalization is small, but it has a dominant effect on SOC.[3e]

According to the model of two-electrons-in-two-orbitals, the energies of the three singlet states S_0, S_1, and S_2 are determined by four independent parameters of the electronic interaction matrix (eq 3), namely, the exchange integral (K_{AB}), the coulomb integral function (K'_{AB}), and the covalent (γ_{AB}) and the polarizing (δ_{AB}) perturbations. The parameter δ_{AB} represents the difference between the basis energies of orbitals A and B ($\delta_{AB} \cong \delta\alpha$ in Hückel theory), and the former corresponds to twice the resonance integral used in semiempirical models ($\gamma_{AB} \cong 2\beta$, cf. ref 3 for details).

$$
\begin{array}{c}
{}^1|A^2 - B^2\rangle \\
{}^1|A^2 + B^2\rangle \\
{}^1|AB\rangle
\end{array}
\begin{pmatrix}
2K'_{AB} & \delta_{AB} & 0 \\
\delta_{AB} & 2(K'_{AB} + K_{AB}) & \gamma_{AB} \\
0 & \gamma_{AB} & 2K_{AB}
\end{pmatrix}
\quad (3)
$$

where

$$\gamma_{AB} = 2\,h_{AB} + (AA|AB)^* + (BB|BA)$$

$$\delta_{AB} = h_A - h_B + (J_{AA} - J_{BB})/2$$

and

$$K'_{AB} = [(J_{AA} + J_{BB})/2 - J_{AB}]/2$$

Diagonalization of the matrix (3) yields the three singlet state wave functions as linear combinations of three basis wave functions ${}^1|AB\rangle$, ${}^1|A^2 + B^2\rangle$ and ${}^1|A^2 - B^2\rangle$, the eigenfunctions of the "perfect" diradical ($\delta_{AB} = \gamma_{AB} = 0$). The first represents the *covalent* (dot-dot) state, and the latter two describe the *zwitterionic* (hole-pair) states. The one-electron SOC Hamiltonian mixes only the symmetrized zwitterionic ${}^1|A^2 + B^2\rangle$ wave function with the triplet state ${}^3|AB\rangle$, and the interaction term is directly proportional to C_+, the coefficient of the wave function ${}^1|A^2 + B^2\rangle$ in the ground state S_0 of the singlet diradical: $|S_0\rangle = C_0{}^1|AB\rangle + C_+{}^1|A^2 + B^2\rangle + C_-{}^1|A^2 - B^2\rangle$.[3] According to Fermi's Golden Rule,[3b,6c] the transmission factor A_{SOC} of eq 2 should then be proportional to the square of this interaction term, eq 4.

$$A_{\mathrm{SOC}} \propto C_+^2 \qquad (4)$$

We assume that the two parameters K_{AB} and K'_{AB} are constant for the series of diradicals **1** and **2** due to their similar topology. This is supported by semiempirical calculations (AM1, see next section), which gave values within $K_{AB} = 0.0074 \pm 0.0012$ eV and $K'_{AB} = 1.58 \pm 0.03$ eV for all geometry-optimized (planar) model diradicals. The effects of the substituents X and Y are, thus, represented by the covalent (γ_{AB}) and polarizing (δ_{AB}) perturbations. The coefficient C_+ is obtained by diagonalization of the interaction matrix, eq 3, for each value of the parameters γ_{AB} and δ_{AB}, and the dependence of C_+^2 on these two parameters is presented in Figure 4 along with the three singlet-state energies, which represent the energy eigenvalues. All energies are defined relative to that of the triplet state ($E_T \equiv 0$ eV), such that the energy of the lowest singlet state of the perfect diradical is $2K_{AB} > 0$.

Consider the slopes of the C_+^2-surface starting from the perfect diradical ($\delta_{AB} = \gamma_{AB} = 0$) in the lower left edge of the upper diagram of Figure 4. The slope along the δ_{AB} axis remains 0 until δ_{AB} reaches the value δ_{crit} (eq 5), at which the weight of the ionic-state contribution rises abruptly to its maximal value, $C_+^2 = {}^1/_2$; in contrast, the C_+^2-surface rises continuously along the γ_{AB} axis. This behavior becomes self-evident by inspection
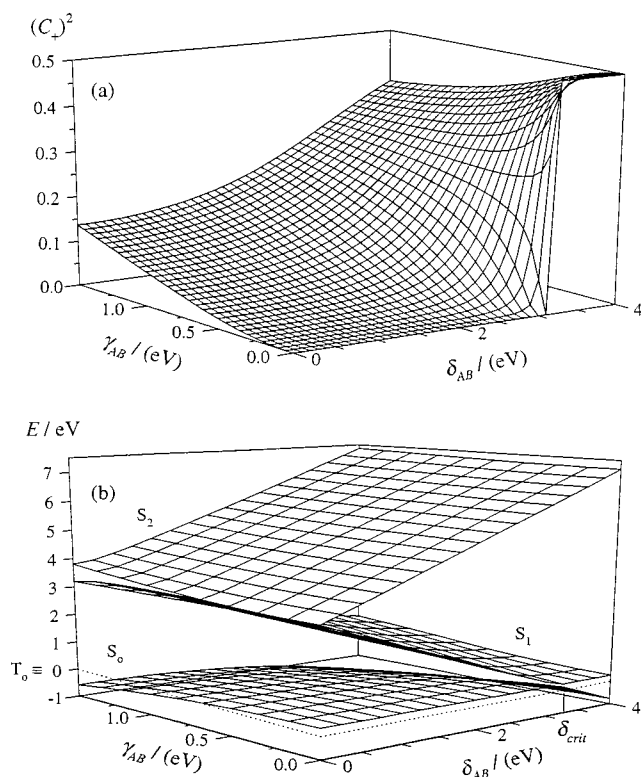

Figure 4. Dependence of (a) the coefficient C_+^2 and (b) the energy of the three singlet states on the electronic parameters γ_{AB} and δ_{AB} with fixed values of $K_{AB} = 0.007$ eV and $K'_{AB} = 1.58$ eV.

of the interaction matrix, eq 3: the polarizing perturbation δ_{AB} mixes only the two zwitterionic wave functions ${}^1|A^2 + B^2\rangle$ and ${}^1|A^2 - B^2\rangle$ and the lowest singlet state S_0 is not affected. At $\delta_{AB} = \delta_{\mathrm{crit}}$ the zwitterionic singlet crosses the covalent singlet state (lower diagram in Figure 4), and the electronic properties of the lowest singlet state S_0 change abruptly. Note that δ_{crit} amounts to 3.17 eV and is far beyond the range of δ_{AB} covered by the aryl substituents, which are used in this work (Table 1). Direct mixing of ${}^1|A^2 + B^2\rangle$ and ${}^1|AB\rangle$ is induced only by the perturbation γ_{AB}, and the nonzero slope along the axis γ_{AB} derives from this coupling of the zwitterionic and covalent wave functions.

$$\delta_{\mathrm{crit}} = \sqrt{K'_{AB}(K'_{AB} - K_{AB})} \qquad (5)$$

The model discussed above provides a simple, qualitative rationale for the empirical relation to the substituent constants σ^+ that is displayed in the Hammett plot (Figure 3). The substituents' electronegativity, which is represented by the parameters σ^+, influences the nonbonding orbital energies (ionization energies)[26] for the corresponding benzyl-type radical fragments A and B. The fact that homosymmetric and nonsymmetric diradicals follow the same trend demonstrates that polar perturbations δ_{AB}, that is, differences in the basis energies of donor- and acceptor-substituted radical centers, hardly influence the ISC rate constants, as predicted by the model. The observed trend must, therefore, arise from the covalent perturbation γ_{AB}, which appears to be related to the sum of the substituent constants, $\sigma_A^+ + \sigma_B^+$. This relation is explained by the qualitative orbital interaction diagram shown in Figure 5. Electron-accepting substituents, for example, NO$_2$, lower the basis energy of the nonbonding molecular orbitals (NBMO's)

(26) (a) Sim, B. A.; Milne, P. H.; Griller, D.; Wayner, D. D. M. *J. Am. Chem. Soc.* **1990**, *112*, 6635. (b) Wayner, D. D. M.; Sim, B. A.; Dannenberg, J. J. *J. Org. Chem.* **1991**, *56*, 4853.
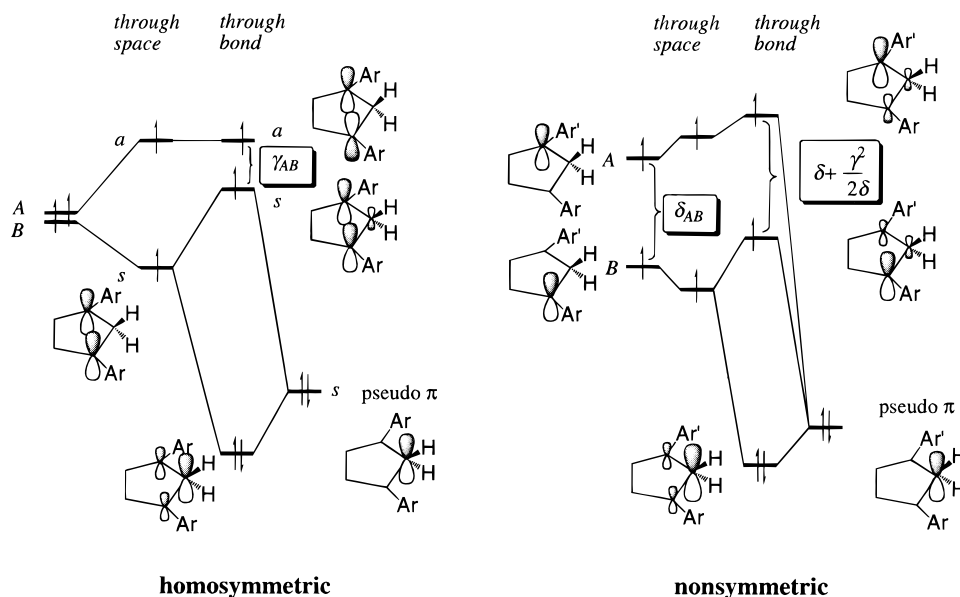
Figure 5. Orbital interaction diagram for the NBMO's in homosymmetric and nonsymmetric diradicals. The symbols a (antisymmetric) and s (symmetric) refer to the symmetry properties of the molecular orbitals with respect to the plane of symmetry that is orthogonal to the plane of the ring in the homosymmetric diradicals; A and B refer to the localized nonbonding molecular orbitals.

and thereby enhance the through-bond interaction of the symmetric NBMO with the lower-lying pseudo π orbital of the methylene bridge[27,28] because the energy gap between the interacting orbitals is reduced (second-order perturbation theory). Conversely, electron-donating substituents, for example, MeO, tend to decrease the through-bond interaction with the pseudo-π orbital. Because of the counteracting effect of the through-space and through-bond interactions, the covalent perturbation γ_{AB}, which corresponds to the resulting energy gap between the NBMO's, increases with decreasing through-bond interaction. As a result, the weight of the zwitterionic wave function $^1|A^2 + B^2\rangle$ increases with the donating ability of the substituents and the rate of ISC increases accordingly (eqs 2 and 4).

Molecular Dynamic Aspects of ISC and Calculation of SOC. The fact that the decay of the triplet diradicals **1** and **2** is associated with activation energies suggests that ISC requires some distortion from the equilibrium geometry. Apart from the weight of the ionic contribution C_+ in the lowest singlet state wave function of the diradicals, the size of the SOC matrix element depends on the relative orientation of the two radical centers, and the one-electron coupling terms vanish for the planar conformation of 1,3-cyclopentanediyl.[2] A natural choice for a reaction coordinate that will facilitate ISC by effective coupling of the singlet and triplet states is the soft ring puckering distortion represented by the dihedral angle Θ shown in the right-hand structure **7** below.
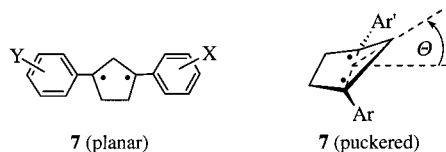
Quantitative evaluation of γ_{AB} was done for the model structures **7**. Geometries were optimized by UHF calculations for the triplet state using the semiempirical AM1 method.[29a,b] The optimized structures were planar (C_{2v}-symmetry for X = Y and C_s-symmetry for X ≠ Y, $\Theta = 0$). Although SOC strength

vanishes in planar geometries, the zwitterionic state contribution C_+ is not 0. The wave functions and energies of the three lowest singlet states at this geometry were then determined by 3×3 configuration interaction (CI). The energy gap between the UHF NBMO's, $\Delta\epsilon$, corresponds to the covalent perturbation γ_{AB} in homosymmetric diradicals. The eigenvalues resulting from diagonalization of the lower right 2×2 block in the interaction matrix, eq 3, are well approximated by second-order perturbation theory, because $\gamma_{AB} \ll 2K'_{AB}$. Hence, the coefficient C_+ in the perturbed electronic ground state S_0 is predicted to be proportional to γ_{AB}, eq 6. In nonsymmetric diradicals the NBMO

$$C_+ \approx \frac{\gamma_{AB}}{2K'_{AB}} \tag{6}$$

energy gap $\Delta\epsilon$ is no longer equal to γ_{AB} (cf. the interaction diagram, Figure 5), but the coefficient C_+ can be determined by orthogonal transformation of the S_0 wave function to the basis set of the localized NBMO's A and B, and eq 6 is still valid.

The values of γ_{AB} that were calculated by the procedure described above are small as a result of the near cancellation of the through-space and through-bond interactions between the radical sites (Figure 5). In such a situation, the relative ordering of the two NBMO energies predicted by a particular model is largely fortuitous.[30] AM1 predicts the symmetric NBMO to lie

(27) (a) Hoffmann, R. *Acc. Chem. Res.* **1971**, *4*, 1. (b) Paddon-Row: M. N. *Acc. Chem. Res.* **1982**, *15*, 245. (c) Goldberg, A. H.; Dougherty, D. A. *J. Am. Chem. Soc.* **1983**, *105*, 284.

(28) The through-bond interaction is due mainly to conjugation through the *pseudo-π* orbital of the methylene bridge, which affects only the symmetric orbital (Figure 5). The ethylene bridge can be ignored in the orbital-interaction diagram because it influences the symmetric and asymmetric NBMOs in a similar manner.

(29) Semiempirical: (a) Dewar, M. J. S.; Zoebisch, E. G.; Healy, E. F.; Stewart, J. J. P. *J. Am. Chem. Soc.* **1985**, *107*, 3902. (b) Rauhut, G.; Chandrasekhar, J.; Alex, A.; Steinke, T.; Clark, T. Vamp, Version 5.0. University of Erlangen-Nürnberg, 1993. Ab initio: (c) Single-point calculations were performed to obtain the triplet (ROHF method) and singlet [CASSCF(2,2)] energies. (d) Frisch, M. J.; Trucks, G. W.; Head-Gordon, M.; Gill, P. M. W.; Wong, M. W.; Foresman, J. B.; Johnson, B. G.; Schlegel, H. B.; Robb, M. A.; Replogle, E. S.; Gomperts, R.; Andres, J. L.; Raghavachari, K.; Binkley, J. S.; Gonzalez, C.; Martin, R. L.; Fox, D. J.; Defrees, D. J.; Baker, J.; Stewart, J. J. P.; Pople, J. A. Gaussian 92, Revision F.4. Gaussian, Inc., Pittsburgh, PA, 1992.

(30) Bieri, G.; Heilbronner, E.; Kloster-Jensen, E.; Schmelzer, A.; Wirz, J. *Helv. Chim. Acta* **1974**, *57*, 1265.
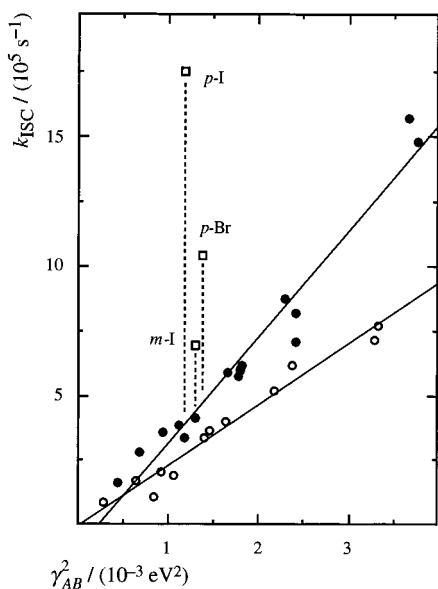
Figure 6. Experimental intersystem-crossing rate constants (k_{ISC}) of diradicals **1** (●) and **2** (○) versus the covalent perturbation (γ_{AB}) of the planar diradicals **7**. The derivatives substituted with bromine or iodine (□) were excluded from the regression analysis, since they exhibit higher ISC rate constants due to the heavy-atom effect.

Figure 7. Parameters γ_{AB}, δ_{AB}, and C_+ calculated for homosymmetric (○) and nonsymmetric (●) diradicals **7** with the same substitution pattern as diradicals **2**.

slightly above the antisymmetric one in the planar diradicals **7** ("reverse" order), in contrast to the "natural" order shown in Figure 5a. An ab initio calculation (STO-3G)[29c,d] for diradical **7** (X = Y = H, C_{2v}) gave the natural orbital energy sequence.

The AM1 calculations were then repeated for various fixed values of the dihedral angle Θ (0°–40°, 5°-intervals). The through-space overlap of the nonbonding orbitals increases with increasing values of Θ, and as a result, the natural orbital energy sequence is restored around $\Theta \approx 24$° for all model compounds **7**. At higher values of Θ the energy gap increases monotonically, and the ratios between the γ_{AB} values obtained for different substituents remained largely constant. The AM1 method is known to underestimate through-space interactions systematically.[12a,31] Instead of chosing some arbitrary value $\Theta > 24$° for our calculations, we scaled the AM1 model by deducing a constant value $\Delta\gamma \approx 0.11$ eV[32] from the covalent perturbations calculated at the planar geometry, $\gamma_{AB} = |\gamma_{AM1} - \Delta\gamma|$ (Table 1), thereby restoring the natural orbital sequence for all compounds.

Effect of Polarizing Substitution. Figure 6 shows that the rate constants k_{ISC} increase linearly with γ_{AB}^2, as predicted by the model of two-electrons-in-two-orbitals (eqs 4 and 6). The polarizing perturbations δ_{AB} appear to have no perceptible influence: nonsymmetric and even push–pull substituted diradicals obey the same linear relationship with γ_{AB}^2 as the symmetric ones. Even for the strong push–pull substitution pattern in compound **1** (X = *p*-OMe, Y = *p*-NO$_2$), the polarizing perturbation, $\delta_{AB} = 0.58$ eV, is well below the critical value, $\delta_{crit} = 3.17$ eV, such that it has no noticeable influence on SOC.

To demonstrate the dominance of the covalent perturbation on the zwitterionic-state contribution (C_+), we redraw in Figure 7 that section of the surface showing the variation of C_+^2 as a
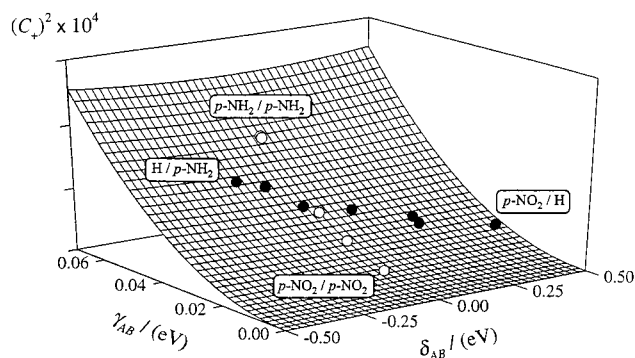
function of δ_{AB} and γ_{AB}, which is actually spanned by the diradicals studied in this work. The parameters are those calculated by AM1 for the model systems **7** (Table 1). In the homosymmetric case (empty circles), the polar perturbation (δ_{AB}) is 0, and the highest zwitterionic-state contribution pertains to the diradical with two amino groups, the lowest value to the derivative with two nitro groups. The polar perturbation reaches substantial values in the donor–acceptor substituted, nonsymmetric derivatives (filled circles), as seen from the displacement to the left and right of the $\delta_{AB} = 0$ line in Figure 7. Nevertheless, SOC depends on the covalent perturbation γ_{AB} only.

In contrast to these findings, ISC rates *do* respond to strong polarizing perturbations δ_{AB} in *para*-substituted singlet phenyl nitrenes, as was recently reported by Gritsan et al.[33] Remarkably, both observations are consistent[34] with Michl's model of two electrons in two orbitals.[3]

Temperature Dependence and Substituent Effects on the Arrhenius Parameters. The ISC rate constants of diradicals **1** and **2** obeyed Arrhenius relations (eq 1) in the range of 10–50 °C, and the parameters ln *A* and E_a were determined by linear regression of $\ln(k_{ISC})$ vs $1/T$ (Table 1). The substituents X and Y give rise to substantial variation in these parameters, and the substituent effects on the two parameters are correlated: large pre-exponential factors tend to be compensated by large activation energies (Figure 8a).

Such correlation between the Arrhenius parameters E_a and ln *A*, or between the equivalent pair of Eyring parameters $\Delta H^\ddagger$ and $\Delta S^\ddagger$, is a common phenomenon.[35] *Enthalpy–entropy compensation* (EEC) (eq 7) and rate-equilibrium *linear free*

$$\delta_R E_a = R\beta\delta_R \ln(A/s^{-1}) \qquad (7)$$

energy relationships (LFERs) (eq 8) are related,[36] so-called

$$\delta_R \ln(k/s^{-1}) = \alpha\delta_R\Delta G^\ominus/RT \qquad (8)$$

extra-thermodynamic relationships.[37] They are encountered regularly in series of compounds such as **1** and **2**, in which aryl substituents remote from the reaction center are varied. In eqs

(31) Comments by Prof. T. Bally, University of Fribourg, in the discussion following a paper of Rauhut, G.; Clark, T. *J. Chem. Soc., Faraday Trans.* **1994**, *90*, 1783.

(32) The precise values of the corrections $\Delta\gamma$ were determined by nonlinear least-squares fitting of eq 9 (see below), where γ_{AB} is substituted by $|\gamma_{AM1} - \Delta\gamma|$. This procedure gave $\Delta\gamma = 0.115 \pm 0.003$ eV for diradicals **1** and 0.114 ± 0.003 eV for diradicals **2**.

(33) Gritsan, N. P.; Tigelaar, D.; Platz, M. S. *J. Phys. Chem. A* **1999**, *103*, 4465.

(34) Referring to the interaction matrix, eq 3, two limiting cases of perfect diradicals may be distinguished: $K_{AB} = 0$ (*pair diradicals*) and $K'_{AB} = K_{AB}$ (*axial diradicals*). Diradicals **1** and **2** approach the first case and have a large value of δ_{crit} (eq 5), as discussed above. Phenylnitrenes, on the other hand, are closer to the second case (in methylnitrene the condition $K'_{AB} = K_{AB}$ is imposed by the three-fold axis of symmetry). Therefore, δ_{crit} is expected to be small, and moderate polar perturbations δ_{AB} *are* expected to increase the ionic contributions to the ground-state singlet wave function of nonplanar phenylnitrenes by second-order interactions.

(35) Leffler, J. E. *Chem. Rev.* **1955**, *55*, 1202.

$\log(A/\text{s}^{-1})$

(a)

$E_a / (\text{kcal mol}^{-1})$

$\log(A/\text{s}^{-1}) - 2\log(\gamma_{AB}/10^{-2}\ \text{eV})$
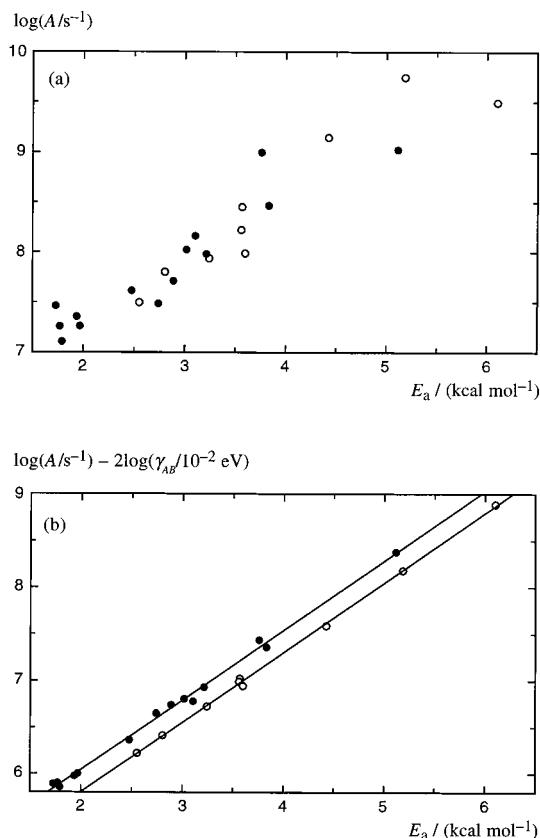
(b)

$E_a / (\text{kcal mol}^{-1})$

Figure 8. Arrhenius parameters log A (upper diagram a) and log A_Δ (eq 9, lower diagram b) versus activation energies E_a for ISC of diradicals **1** (●) and **2** (○).

7 and 8 we use the notation of Leffler and Grunwald:[37a] the operator δ_R denotes the change in the subsequent quantity caused by the substituent R, for example, $\delta_R\Delta G^\ominus = \Delta G^\ominus[\text{R} = \text{X}] - \Delta G^\ominus[\text{R} = \text{H}]$. A series of compounds adhering to eq 7 is also said to obey an *isokinetic relationship* (IKR), because eq 7 implies that the dependence of the rate constants on substitution defined by eq 1, $\delta_R \ln(k/\text{s}^{-1}) = \delta_R \ln(A/\text{s}^{-1}) - \delta_R E_a/RT$, vanishes for $T = \beta$. The parameter β is called the *isokinetic temperature*, the temperature at which all compounds of the series react with the same rate, and where all Arrhenius plots intersect. The slope α in eq 8 is commonly called the *Brønsted parameter.*

Let us return to the extended Arrhenius relation, eq 2. From eqs 4 and 6 we know that the first factor A_{SOC} is proportional to γ_{AB}^2, so we may as well define $A_{\text{SOC}}/\text{s}^{-1} \equiv (\gamma_{AB}/\text{eV})^2$ and leave the proportionality factor to A_Δ. When $\ln A_\Delta = \ln A - 2 \ln \gamma_{AB}$ is plotted against E_a, most of the scatter in Figure 8a is eliminated and the data separate into two accurately linear relations, eq 9, for the two sets of diradicals **1** and **2** (Figure

$$\delta_R \ln(A_\Delta/\text{s}^{-1}) \equiv \delta_R \ln(A/\text{s}^{-1}) - 2\delta_R \ln(\gamma_{AB}/\text{eV}) = \delta_R E_a/R\beta \tag{9}$$

8b).[38] This suggests that the factor $A_\Delta \exp(-E_a/RT)$, which reflects thermal activation, obeys EEC, $\delta_R E_a = R\beta\delta_R \ln(A_\Delta/\text{s}^{-1})$.

Before we proceed to an interpretation of these results, we must pause to establish that the apparent EEC exhibited by the series of compounds **1** and **2** is statistically significant. That proved to be rather involved, and although the general problem has received considerable attention in the literature,[39–42] we found that an adequate test for EEC had not been described. Readers who are willing to accept our assertion that the correlations depicted in Figure 8b are highly significant and who are not interested in the intricacies of the statistical analysis may skip the next section.

Statistical Analysis of the Enthalpy−Entropy Compensation (EEC). Since Leffler published his classical review article on enthalpy−entropy relationships,[35] the statistical analysis of such data has been discussed extensively.[39–42] The issue is a delicate one because the experimental errors of the Arrhenius parameters are strongly correlated: even in the absence of any correlation between the expectation values (the "true" values) of E_a and $\ln A_\Delta$, their estimators $\hat{E}_a$ and $\ln \hat{A}_\Delta$, which are obtained by linear regression, will be correlated, and the expectation value of the correlation coefficient $\rho(\hat{E}_a, \ln\hat{A}_\Delta)$ will approach unity as the experimental temperature range becomes small. Moreover, large experimental errors tend to raise the correlation coefficient $\rho(\hat{E}_a, \ln \hat{A}_\Delta)$ rather than lower it. Therefore, the mere observation of correlation between estimated Arrhenius parameters of a reaction series (as in Figure 8b) cannot, by itself, be taken as evidence for the existence of an IKR. Furthermore, correlation arising purely from the covariance of the random errors will suggest an apparent isokinetic temperature that is close to the harmonic mean of the experimental temperatures, $\beta \approx \langle 1/T\rangle^{-1}$,[41] and one is well advised to be especially suspicious when the apparent isokinetic temperature lies near the experimental temperatures, as in the present case.

Two methods have been described to test for the existence of an IKR,[40,41] and it was reported[42a] that they give essentially the same results. We have used the method of Exner:[40] linear regressions of experimental Arrhenius plots are done (i) individually for each compound and (ii) under the IKR constraint that all the regression lines intersect at some temperature $T = \beta$. As β is not known a priori, the residual sum of squares is calculated for trial values of β until the minimum, S_0, is found. This is compared to the residual sum of squares that is obtained when a separate straight line is fitted to the data of each compound without any restriction, S_{00}. An F-statistic, eq 10, is

$$F(f_0, f_{00}) \approx \frac{(S_{00} - S_0)/f_0}{S_{00}/f_{00}} \tag{10}$$

calculated to test the *isokinetic hypothesis*, that is, the *null hypothesis* H_0: the true (error-free) regression lines of all compounds intersect at one point. It is assumed that the F-test is not sensitive to the fact that the relation between the two

(36) The existence of a LFER *implies* the existence of EEC, if the temperature dependences of the activation enthalpy $\Delta H^\ddagger$ and entropy $\Delta S^\ddagger$ are negligible in the range covered by the experimental data (ref 37a, pp 155−161). EEC is sometimes used in a qualitative sense. If it implies an exact linear relation between $\Delta H^\ddagger$ and $\Delta S^\ddagger$ (or E_a and $\ln A$, eq 7), then EEC and IKR are synonymous.

(37) (a) Leffler, J. E.; Grunwald, E. *Rates and Equilibria of Organic Reactions*; Wiley: New York, 1963. (b) Hammett, L. P. *Physical Organic Chemistry. Reaction Rates, Equilibria, and Mechanisms*; McGraw-Hill: New York, 1970. (c) Grunwald, E. *Thermodynamics of Molecular Species*; Wiley: New York, 1997.

(38) The ISC rates of heavy-atom substituted derivatives (Br and I) were substantially faster than predicted by the model function (cf. Figure 6) and were omitted from this analysis. Derivatives containing cyano substitutents consistently had ISC rates somewhat less than expected. This is attributed to the parametrization of the AM1 model, as the calculated orbital energies also fell out of line with the corresponding Hammett substituent constants or ionization energies. The cyano-substituted derivatives were, therefore, also omitted, but their inclusion would not have had a substantial effect on the overall results. Note that eq 9 implicitly contains $\Delta\gamma$ as an adjustable parameter (ref 32), which is used to calculate γ_{AB} from the AM1 interaction terms γ_{AM1} given in Table 1.

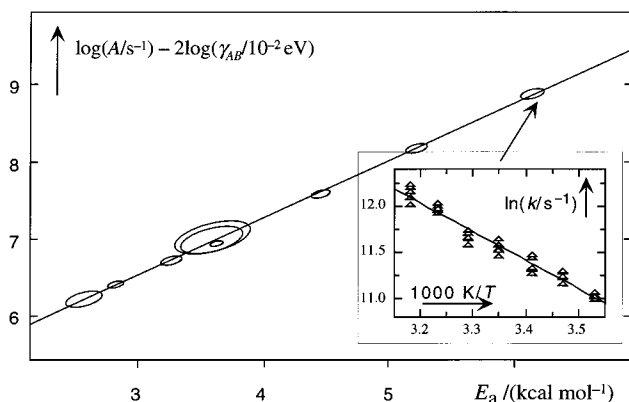(39) Petersen, R. C. *J. Org. Chem.* **1964**, *29*, 3133.

Figure 9. Correlation diagram of the Arrhenius parameters log A_Δ and E_a for diradical **2** with 95% confidence regions. Each of the data points (at the center of the confidence regions, not shown for clarity) was obtained as the slope and intercept of an Arrhenius plot. The inset shows the plot for **2** (X = Y = NO_2) as an example. Note that the long axes of the elliptic confidence regions are approximately parallel to the regression line. The ellipses are a pictorial representation of the random-error contribution to the correlation of the Arrhenius parameters. The total variation in the data is much larger than that arising from random error. The plot for diradicals **1** is similar (not shown).

models is not accurately linear.[43] The degrees of freedom of the unconstrained regression (i) are f_{00} = number of data points − 2(number of compounds), and those associated with introducing constraint (ii) are f_0 = number of compounds − 2.

The SOC-adjusted rate constants, $k' = k/(\gamma_{AB}/eV)^2$, for the two reaction series, diradicals **1** (14 compounds, 878 data points) and **2** (9 compounds, 486 data points), were analyzed by Exner's method, which gave $\beta = 273$ K and $F(12, 850) = 9.0$ for **1** and $\beta = 285$ K and $F(7, 468) = 20.9$ for **2**. Both of these F-statistics are much larger than the corresponding values of the two-tailed F-distribution at a significance level of >99% [$F(12, 850) = 2.2$, $F(7, 468) = 2.66$]. Therefore, H_0 must be rejected. The residual variance of the unconstrained model is lower than that of the isokinetic model at a confidence level of >99%. We are forced to conclude that the lines defined by eq 11 do *not* intersect

$$\ln(k'/s^{-1}) = \ln(k/s^{-1}) - 2\ln(\gamma_{AB}/eV) = \ln(A_\Delta/s^{-1}) - E_a/RT \tag{11}$$

at a single point, that is, that the expectation values of the regression parameters E_a and ln A_Δ do *not* obey the isokinetic relationship, eq 9.

However, the (elliptic) 95% confidence regions of the data pairs (E_a, ln A_Δ) are much smaller than their total variation (Figure 9), and that indicates that enthalpy−entropy compensation (EEC) is real. How can these two views be reconciled? We should not expect an IKR to hold *exactly* because it is an extra-thermodynamic relationship that does not have a sound physical basis. Moreover, large sample sizes will lead one to reject any null hypothesis, H_0, that is not exactly true because a huge sample will reduce the standard error to the point where

(40) Exner, O. In *Progress in Physical Organic Chemistry*; Wiley: New York, 1973; Vol. 10, p 411.

(41) Krug, R. R.; Hunter, W. G.; Grieger, R. A. *J. Phys. Chem.* **1976**, *80*, 2335 and 2341.

(42) (a) Linert, W.; Jameson, R. F. *Chem. Soc. Rev.* **1989**, *18*, 477. (b) Linert, W. *Chem. Soc. Rev.* **1994**, 429.

(43) The restricted model (ii) is not simply defined as a submodel of (i) by the linear eq 11 because β is estimated simultaneously with the parameters $\ln(A')$ and E_a.

Table 2. Estimators and Credible Intervals for the Isokinetic Temperature β and for the Correlation Coefficient ρ between the Expectation Values of the Arrhenius Parameters ln A_Δ and E_a Determined by Gibbs Sampling (Appendix II)

parameter	percentiles of the (re-sampled) posterior distribution (10000 iterations)		
	2.5%	50% (median)	97.5%
$\beta(\mathbf{1})/K$	301	292	281
$r(\mathbf{1})$	−0.9988	−0.9982	−0.9975
$\beta(\mathbf{2})/K$	300	291	281
$r(\mathbf{2})$	−0.9995	−0.9994	−0.9991

even a minuscule difference becomes statistically discernible. That is, H_0 may be rejected although it is practically true.[44]

The essential first step is to ask the proper question. Above we asked whether the data are consistent with an exact IKR, and the answer was No. However, we may still be interested to know whether the true (error-free) Arrhenius parameters are *correlated*, that is, whether EEC, an *approximate* IKR, exists and how strong that linear association is. To answer this question, we need to know whether the observed correlation between the two parameters, E_a and ln A_Δ, exceeds that expected on the basis of purely random errors in the data.

We propose two treatments to answer this question, a quick-and-dirty method given in Appendix I and a more sophisticated treatment, which is based on Bayesian inference and uses Gibbs sampling, in Appendix II. The conclusion from both treatments is the same: now, the hypothesis cannot be rejected because we have made a weaker claim. We do not imply the existence of an *exact* IKR in the sense that all of the true Arrhenius lines must intersect at a single point, but we do claim that the expectation values of E_a and ln A_Δ are strongly correlated. Estimated correlation coefficients between the expectation values of E_a and ln A_Δ obtained by the two methods are similar, and both are very high ($r^2 > 0.99$). In addition, the second method provides estimates of the parameters E_a and ln A_Δ and of the isokinetic temperature β with credible intervals (a Bayesian analogue to confidence intervals: 2.5% and 97.5% percentiles of the resampled posterior distributions). The values of β determined in this way for the series **1** and **2** (Table 2), are nearly the same, $\beta = 291 \pm 10$ K, and similar to the β-values obtained by the method of Exner. However, the interpretation of β is now different: it is the temperature where we have maximum, though not perfect, EEC. The 2-dimensional "coordinates" of the "isokinetic" point, β and $\ln(k_0)$, now represent the mean of a bivariate normal distribution. The resulting credible intervals of the Arrhenius parameters are reproduced in Table S2 of the Supporting Information. They are very similar to the standard errors given in Table 1 that were obtained by independent linear regression for each compound.

Toward an Intuitive Understanding of Substituent and Temperature Effects on Diradical Lifetimes. The π-orbitals of the sp² radical centers are parallel in the planar conformation of cyclopentane-1,3-diyl diradicals, and their conformational mobility is restricted. According to Salem and Rowland's first rule,[2] SOC vanishes for parallel π-orbitals, and this is held responsible for the relatively high persistence of triplet cyclopentane-1,3-diyl diradicals such as **1** and **2**, which are stable for hours at 77 K and decay on the microsecond time scale at room temperature in solution. The pattern of substituent and temperature effects on these lifetimes is rather complex. Examination of the data in Table 1 reveals that activation

(44) For example, Wonnacott, T. H.; Wonnacott, R. J. *Introductory Statistics*, 3rd ed.; Wiley: New York, 1977.
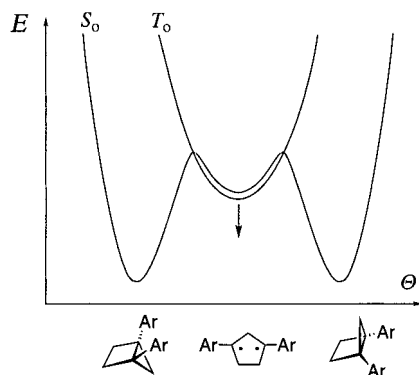
Figure 10. Singlet and triplet potential-energy surfaces of diradical **7** along the out-of-plane bending mode defined by the dihedral puckering angle Θ (see structure **7** in the text).

energies and SOC strengths are not related. Both electron-withdrawing (nitro) and electron-donating (amino) substituents lower the activation energies in diradicals **1** and **2** compared to the parent compound. Such behavior is indicative of a radical-stabilizing effect of the substituents.[45] Nevertheless, the lifetimes determined at ambient temperature exhibit a monotonic increase with increasing electron-withdrawing properties as expressed by, for example, Brown's substituent constants σ^+ (Figure 3).

The aryl-stabilized diradicals **1** and **2** are real minima rather than transition states (Figure 10). An energy barrier of 2−3 kcal mol^{-1} has been determined experimentally for ring closure of the singlet diradical **7**(X = Y = H) to diphenylhousane.[21] The triplet diradical lies somewhat below the singlet diradical [ΔE_{ST} ∼0.5 kcal mol^{-1} by AM1, 3 × 3 CI,[29a−c] or STO-3G)[29c,d]], which further enhances the total activation energy required for housane formation from the triplet diradical. Aryl substituents cause various degrees of radical stabilization. Hence, donor *and* acceptor substituents stabilize the singlet and triplet diradicals relative to the housane (vertical arrow in Figure 10) and increase the activation energies for intersystem crossing.

The simple empirical *Ansatz* expressed in eq 2 successfully deals with the present case of a thermally activated reaction that is inhibited by a spin barrier. The probability of ISC appears in a transmission factor A_{SOC} that is modeled by SOC strength. The "standard" Arrhenius term $A_\Delta \exp(-E_a/RT)$ describes thermal activation in the same way as for a spin-allowed reaction, and it obeys the structure−reactivity rules expected for an aryl reaction series. The fact that the lifetimes of diradicals **1** and **2** at room temperature are largely explained by considering only the factor A_{SOC} now appears to be rather coincidental and due to the approximate isokinetic relationship obeyed by the parameters $\ln A_\Delta$ and E_a: the isokinetic temperatures happen to lie close to room temperature, such that the substituent effects arising from the term $A_\Delta \exp(-E_a/RT)$ largely cancel.

Conclusions

This work represents an extensive study of substituent effects on a reaction series in which the rate-determining step involves ISC. The rate constants for ring closure of the triplet 1,3-cyclopentanediyl diradicals **1** and **2** at room temperature are affected in a systematic manner by substituent variation. Analysis within the frame of a two-electrons-in-two-orbitals active space indicates that the substituent effects on these rate constants are well described by the magnitude of SOC, which can be easily calculated from the zwitterionic-state contribution

(C_+) in the electronic wave function of the diradical's lowest singlet state S_0. As predicted for nonaxial diradicals,[3] SOC is insensitive to donor−acceptor substitution but is enhanced by through-bond interaction. The systematic variation of the ISC rate constants with Brown's σ^+ substituent constants reflects the through-bond interaction of the nonbonding orbitals, which increases with the electron-withdrawing propensity of the substituents.

The temperature coefficients of the ISC rate constants exhibit strong enthalpy−entropy compensation (EEC). The isokinetic temperature β of the thermally activated process happens to be near room temperature in this reaction series. Thus, the effect of substituents on the activation energy for cyclization is largely canceled by EEC at room temperature, which results in the deceptively simple relationship between ISC rate constants and the calculated magnitude of SOC, $k_{ISC} \propto C_+^2$.

Appendix I

Let the logarithms of rate constants k'_{ij}, measured at inverse temperatures $\theta_{ij} = 1/T_{ij}$, be linearly related, eq I.1,

$$\log(k'_{ij}) = \alpha_i + \beta_i \theta_{ij} + \epsilon_{ij} \qquad (I.1)$$

where the index i ($i = 1, ..., n$) runs over the n substances B_i, and the index j ($j = 1, ..., n_i$) runs over the n_i measurements done for compound B_i. These n expressions include Arrhenius' law for the systematic part, with $\alpha_i = \ln A_i'$ and $\beta_i = -E_{a,i}/R$, and error terms ϵ_{ij}, which are considered as normally distributed random variables, $\epsilon_{ij} \approx N(0,\sigma_i^2)$. Estimators for the intercepts α_i, a_i, and for the slopes β_i, b_i, are obtained by linear regression of a sample of n_i experimental data pairs (k'_{ij}, θ_{ij}) obtained for each compound B_i. The estimators a_i and b_i of a given compound B_i are correlated, as is well-known from the theory of linear regression, eq I.2.[46a] That correlation arises from the

$$\rho(a_i, b_i) \equiv \frac{cov(a_i, b_i)}{\sqrt{var(a_i)\, var(b_i)}} \qquad (I.2)$$

random error terms ϵ_{ij} in the sample data. As an example, the corresponding 95% ellipsoidal joint confidence regions for the data pairs (a_i, b_i) of compounds **2** are shown in Figure 9.

The correlation between the expectation values α and β is defined by eq. I.3.

$$\rho(\alpha,\beta) = \frac{cov(\alpha,\beta)}{\sqrt{var(\alpha)\, var(\beta)}} \qquad (I.3)$$

Note that eqs I.2 and I.3 address entirely different correlations. Equation I.3 represents the correlation of the *expectation values* α_i and β_i for different substances B_i, the amount of enthalpy−entropy compensation (EEC) in the reaction series. It is not contaminated by the correlation of the estimators, eq I.2, which arises from experimental error. If $\rho(\alpha,\beta)$ is high, that is evidence for a high degree of EEC. Our goal is to obtain an estimate, $r(\alpha,\beta)$, for EEC as defined by eq I.3. To this end, we partition the variances and the covariance of the n estimators, a_i and b_i, $i = 1, ... n$, into two portions, one due to error correlation, eq I.2, and another due to the intrinsic correlation $\rho(\alpha,\beta)$. As estimators for the elements of the variance-covariance matrix of α_i and β_i required in eq I.3, we propose eqs I.4−I.6, in which the contributions arising from error correlation, maxvar(a), maxvar(b), and maxcov(a,b), are subtracted.

(45) Adam, W.; Harrer, H. M.; Kita, F.; Nau, W. M. *Adv. Photochem.* **1998**, *24*, 205.

(46) Draper, N. R.; Smith, H. *Applied Regression Analysis*, 3rd ed.; Wiley: New York, 1998, (a) p 129, (b) p 219.

$$\text{var}(\alpha) = \frac{1}{n-1}\sum_{i=1}^{n}[a_i - \bar{a}]^2 - \text{maxvar}(a) \qquad (I.4)$$

$$\text{var}(\beta) = \frac{1}{n-1}\sum_{i=1}^{n}[b_i - \bar{b}]^2 - \text{maxvar}(b) \qquad (I.5)$$

$$\text{cov}(\alpha, \beta) = \frac{1}{n-1}\sum_{i=1}^{n}[a_i - \bar{a}][b_i - \bar{b}] - \text{maxcov}(a,b)$$

$$(I.6)$$

To obtain a conservative estimate, we take the terms maxvar-(a), maxvar(b), and maxcov(a,b) from the largest variance−covariance matrix of all samples (a_i,b_i), that is, from that with the greatest sum of the two eigenvalues (and the largest ellipsoidal confidence area, cf. Figure 9). If the confidence interval of $r(\alpha,\beta)$ does not contain 0, the null hypothesis H_0: $\rho(\alpha,\beta) = 0$ may be rejected.

Appendix II

We assume n linear Arrhenius relations, eq II.1, defined as in eq I.1.

$$\log(k'_{ij}) = \alpha_i + \beta_i\theta_{ij} + \epsilon_{ij}, j = 1, \dots n_i, \epsilon_{ij} \approx N(0,\sigma_i^2) \quad (II.1)$$

If an exact isokinetic relationship (IKR) existed, the Arrhenius parameters α_i and β_i were related by the set of eqs II.2, where

$$\alpha_i = y_0 - x_0\beta_i \ i = 1, \dots, n \qquad (II.2)$$

$x_0 = 1/\beta$ and $y_0 = \log(k'_{ij})$ at $T = \beta$. The set of eqs II.2 is a recast of eq 11.

As eq II.2 may not hold exactly, in eq II.3 we introduce "error" terms δ_i which are assumed to be distributed according to a normal distribution with expectation 0 and variance τ^2. Note that the errors δ_i do not represent experimental errors. Rather, they represent deviations of the expectation values α_i and β_i from the exact IKR (eq II.2). We now proceed to obtain an estimator $r(\alpha,\beta)$ for the correlation $\rho(\alpha,\beta)$, as defined in eq I.3, Appendix I.

$$\alpha_i = y_0 - x_0\beta_i + \delta_i, i = 1, \dots, n, \delta_i \approx N(0,\tau^2) \quad (II.3)$$

The statistical model is defined by eqs II.1 and II.3 simultaneously. We treat the model in a Bayesian framework.[47] In this context it is indispensable to make an uninformative choice of a priori distributions, the so-called prior distributions, for the model parameters, β_i, σ_i^2, τ^2, x_0, and y_0, that are to be estimated. Diffuse but proper distributions were chosen as priors

Table 3. A Priori Distributions Chosen for Gibbs Sampling

model parameter	prior distribution	parameter values in the prior density
$\alpha_i, \beta_i \ i = 1, \dots n$	normal	$\mu = 0, \sigma^2 = 10^4$
$\sigma_i^2 \ i = 1, \dots n$	gaussian[a]	$r = 0.001, \mu = 0.001$
τ^2	gaussian[a]	$r = 0.001, \mu = 0.001$
(x_0, y_0)	bivariate normal	$\boldsymbol{\mu} = (0,0) \ \mathbf{cov} = \begin{pmatrix} 10^3 & 0 \\ 0 & 10^3 \end{pmatrix}$

[a] $f(x \mid r, \mu) = \mu^r \, x^{r-1} \, e^{-\mu x}/\Gamma(r)$.

for the model parameters (Table 3). Bayesian inference consists of updating prior knowledge about the model parameters by the data, resulting in the so-called posterior densities via the theorem of Bayes: *posterior $\propto$ likelihood $\times$ prior*. All conclusions about the parameters of the model and their functions, such as the correlation ρ, are drawn from the corresponding posterior densities.

The posterior densities given in Table 2 were obtained by Gibbs sampling[48] using the program BUGS.[49] Instead of calculating exact estimates of the posterior distributions, which would mean performing integrations of high dimension, this technique generates a stream of simulated values from the conditional (with respect to the other model parameters) distributions of each model parameter of interest and of functions of the model parameters. The process is iterated (10 000 iterations) until the distributions of the estimated parameters stabilize.

Supporting Information Available: Experimental spectroscopic details, computational procedures, synthesis, and characterization of the four symmetrically substituted azoalkanes **4** (X = Y = *p*-NH₂, *p*-OMe, *p*-CN, *p*-NO₂) and their corresponding housane derivatives **6**, the original kinetic data (Table S1) and more detailed output of the statistical analyses (Table S2). This material is available free of charge via the Internet at http://pubs.acs.org.

(47) Box, G. E. P.; Tiao, G. C. *Bayesian Inference in Statistical Analysis*; Wiley: New York, 1992.

(48) Casella, G.; George, E. I. *Am. Stat.* **1992**, *46*, 167.

(49) Thomas, A.; Spiegelhalter, D. J.; Gilks, W. R. In *Bayesian Statistics*; Bernardo, J. M., Berger, J. O., Dawid, A. P., Smith, A. F. M., Eds.; Clarendon Press: Oxford, U.K., 1992; Vol. 4, p 837. The program and manual are available on the Internet, www.mrc-bsu.cam.ac.uk/bugs.